J Mol Model (2014) 20:2130
DOI 10.1007/s00894-014-2130-y

ORIGINAL PAPER

# Encapsulation of sodium radio-iodide in fullerene $C_{60}$

**Alejandro Valderrama · José Guzman**

Received: 17 July 2013 / Accepted: 27 December 2013 / Published online: 1 March 2014
© Springer-Verlag Berlin Heidelberg 2014

**Abstract** In this work we have studied the well-known "Buckminsterfullerene" $C_{60}$ containing different amounts, from one to four molecules, of sodium radio-iodide ($Na^{131}I$), with density functional theory geometrical optimizations and molecular dynamics at 310 K and atmospheric pressure. We found that nanocapsules with the radioactive content $Na^{131}I@C_{60}$, $2Na^{131}I@C_{60}$ and $3Na^{131}I@C_{60}$ are stable. Furthermore, the $C_{60}$ fullerene undergoes expansion when the number of sodium radio-iodide molecules inside increases. Utilizing the Mulliken charge distribution analysis it was shown that a small charge transfer occurs from iodine to fullerene's carbon atoms. This produces repulsion which increases bond lengths thus the structure is weakened while the binding energy per atom decreases. For the case in which the fullerene initially contains four sodium radio-iodide molecules the expansion is greater than that which the structure can withstand. So the fullerene breaks and releases its contents. This result leads us to conclude that the fullerene can encapsulate up to three molecules of sodium radio-iodide.

**Keywords** Buckyball · $C_{60}$ · Fullerene · Nanocapsule · Sodium radio-iodide

A. Valderrama (✉) · J. Guzman
Centro de Investigación en Ciencia Aplicada y Tecnología Avanzada Unidad Legaria, Instituto Politécnico Nacional, Calzada Legaria No. 694, Colonia Irrigación, Delegación Miguel Hidalgo, 11500 Mexico, DF, Mexico
e-mail: alecvald@gmail.com

A. Valderrama
Facultad de Ciencias, Universidad Nacional Autónoma de México, Avenida Universidad No. 3000, Ciudad Universitaria, Circuito Exterior, Delegación Coyoacán, 04510 Mexico, DF, Mexico

## Introduction

Cancer is a devastating disease that effects the world's population at every level of society [1]. This disease is characterized by the rapid multiplication of abnormal cells that extends beyond the usual limits constituting solid or hematological tumors that invade adjoining parts of the body or spread to other organs, a process known as metastasis. Metastasis is the major cause of cancer death [2]. Current treatments based on radiation therapy and chemotherapeutic drugs affect both diseased cells and healthy cells with no clear distinction between the various human organ tissues in most cases, therefore produces limited effectiveness [3].

As cancer is a cellular disease, in order to combat this invasive disease effectively represents a huge challenge for medicine and new technologies; to study a new generation of drugs that can distinguish cancer patients tissues and perform a targeted medication is vital in the next step for cancer treatment [4]. With the development of nanotechnology it has intensified the study of various possible materials and nanostructures that can be found in nature, laboratories or built [5] for that purpose. Development of materials with precise biomedical function is a growing area of nanotechnology [6]. In this context, carbon nanotubes and fullerenes (spherical nanostructures), have an inherent advantage over other nanomaterials since they allow the encapsulation of compounds in its interior, while biomolecules may be attached on their outer walls to serve as specific molecular recognizers.

Recently there has been considerable experimental research focusing on the use of carbon nanostructures as multifunctional carriers [7]. In particular, single-walled carbon nanotubes (SWNTs) can be filled with a large variety of compounds, ranging from organic molecules [8, 9] to inorganic materials [10]. Sung You Hong and coworkers synthetized SWNTs, which were filled with CuBr or $Na^{125}I$ and then were functionalized. They found that

nanoencapsulation of iodide within single-walled carbon nanotubes enabled its biodistribution to be completely redirected from tissue with innate affinity (thyroid) to lung [11]. Other carbon materials, such as the endohedral fullerenes, can also be filled with smaller numbers of paramagnetic [12, 13] or radio emitting [14] atoms. Also, several theoretical studies have been reported for the encapsulation of transition metal (TM) atoms and clusters inside fullerenes and carbon nanotubes [15–18].

Using DFT [19] calculations, Polina Tereshchuk [20] reported general trends for the encapsulation properties of the $TM_m@C_n$ (TM = Fe, Co, Ni; $m$=2–6, $n$=60, 70, 80, 90) systems. They identified a few physical parameters that play an important role in the sign and magnitude of the encapsulation energy, namely, cluster size, fullerene equatorial diameter, shape, curvature of the inside $C_n$ surface, number of TM atoms that bind directly to the inside $C_n$ surface. In other works, Garg et al. [21], using DFT, studied the encapsulation of 3d atoms inside small fullerenes, $C_n$. They found that the $C_n$ size plays an important role in the magnetic interactions, i.e., the system changes from ferromagnetic (FM) to antiferromagnetic (AFM).

On the other hand, the encapsulation of sodium radio-iodide inside fullerenes would potentially lead to technological uses as an effective way in the treatment of tumors. Based on experimental details [11] as it is commonly performed, it is possible to administer an intravenous concentrated radiodosis for the treatment of hyperthyroidism [22–24]. The alternative is in the encapsulation of sodium radio-iodide that could be redirected within the human body, avoiding the action of its natural thyroid tissue affinity [25]. Hence, the study of the encapsulation of this compound is of great importance. Through this study, it is possible to establish a carbon nanotube's storage capacity limit [26, 27], particularly in the fullerene $C_{60}$ [28] since it largely retains its fundamental molecular properties [29], with respect to the number of $Na^{131}I$ molecules within.

Some important questions in this regard are: which are the interactions between sodium radio-iodide and $C_{60}$? Is it possible to establish a fullerene's storage capacity limit with respect to the number of $Na^{131}I$ molecules within?

The objective in this work is to study the encapsulation capacity of sodium radio-iodide inside $C_{60}$ in the framework of density functional theory (DFT).

## Methods

Density functional theory (DFT) [19, 30] with the generalized gradient approximation (GGA) [31], molecular dynamics (MD) [32], within Born-Oppenheimer approximation and Quantum Espresso code [33] were utilized. For the exchange-correlation energies, the Perdew-Burke-Ernzerhof expression [34] was used. We made use of a norm conserving Martins-Troullier pseudo potentials [35, 36], in the fully separable form of Kleinman-Bylander [37]. Amsterdam density functional (ADF) code was applied to make the Mulliken population analysis and the graphics representations.

The energies of the structures were computed taking the valence electronic states for carbon: $2s^2 2p^2$, for iodine: $5s^2 5p^5$ and for sodium: $2s^2 2p^6 3s^1$. The cut-off energy was 544.22 eV, and we implemented a uniform grid of eight irreducible k-points within the Monkhorst-Pack special k point scheme [38]. To treat partial occupancies we used a Methfessel-Paxton [39] smearing of order 1 and a width of 0.7 eV. The threshold energy convergence was 0.1 meV. These parameters proved adequate for our calculations [40].

We allowed systems to follow an evolutionary process using molecular dynamics, with a temperature of 310 K at one atmosphere of pressure and a time step of 1 femtosecond. We controlled the temperature in the MD calculations via velocity rescaling. The pressure in the Quantum Espresso code is controlled by adding degrees of freedom for the cell size and volume with an application of the Parrinello-Rahman Lagrangian [41].

Scalar relativistic spin polarized and non-spin polarized calculations were performed. In each case, the results were the same. This observation implies that we have non-magnetic systems.

All calculations were performed with an estimated SCF accuracy $< 9.0\times10^{-5}$ eV.

There are different ways to calculate the formation energy of the fullerene $C_{60}$ with various atoms or molecules inside [42]. Some methods consider that the fullerene is formed with atoms which were added one by one or as molecules ($C_2$, $C_3$) and by isomerization of some type of precursor molecule, for example. However the published values by each method usually differ because formation energy, which is intimately related to the thermodynamic stability, is hard to calculate precisely [43, 44].

This study selected density functional theory (DFT) as the best option for accuracy and speed for studying the systems composed of fullerene $C_{60}$ with different number of $Na^{131}I$ molecules contained. For these kinds of systems it was decided to determine the formation energy in an alternative way: we defined the formation energy as $E_{nf} = E(nNa^{131}I@C_{60}) - [60E(C) + nE(Na^{131}I)]$; where $E(nNa^{131}I@C_{60})$ is the energy of the final optimized configuration of the composite system and $[60E(C) + nE(Na^{131}I)]$ is the energy of 60 atoms from a gas of atomic carbons with no interaction between them plus the energy of n isolated molecules of $Na^{131}I$. For $n$=0 we obtain the formation energy of the single fullerene $C_{60}$. Thus, the average binding energy per atom in the fullerene is $E_{0f}/60$. Using this simple formula, we found correct cohesive energy per carbon atom in the fullerene.

Furthermore, in the case of composite systems with 1, 2, or 3 molecules of $Na^{131}I$ contained in the fullerene, the encapsulation energy per molecule of $Na^{131}I$, is $\Delta E_n \approx E_{nf}/(60+2n) * 2$, since each $Na^{131}I$ molecules have two atoms and supposing that their cohesive energy is approximately the same as the other atoms in the system. The calculated results are presented below.

## Results and discussion

### $C_{60}$ fullerene's optimization and molecular dynamics

After 18 calculating cycles, (see Fig. 1) the total energy that corresponds to the minimum $C_{60}$'s molecular energy at ground state, was found to be – 9278.6506 eV. Thus the obtained molecular formation energy is – 427.59 eV, while the average cohesive energy per atom is – 7.13 eV, which differs from the published value by Xinlei Hua et al. [45] by approximately 0.8 %, this confirms the reliability of our method.

As shown in Fig. 1, the fullerene's spherical shell has higher positive potential (dark blue) and contains a near neutral region (light blue), which can store other atoms and molecules. The green illuminated region is practically neutral in the logarithmic scale.

The $C_{60}$ fullerene has several axes of symmetry, the inset of Fig. 1 shows two of them, one in the direction of the double bond at the center of the image, axis of symmetry 1 (AS1), and the other in the perpendicular direction, axis of symmetry 2 (AS2). Note that AS1 crosses the ends of the fullerene parallel to a carbon double bond, while the AS2 crosses the ends of the fullerene through atoms that are at opposite poles. This difference is responsible for equipotential areas that are not distributed with central symmetry, only with respect to these two axes of the fullerene. For this reason this appears in the upper left and lower right edges of the negative red zone. However, there are red areas in the opposite direction, only they are clipped in the figure and cannot be observed because they are slightly more distant.

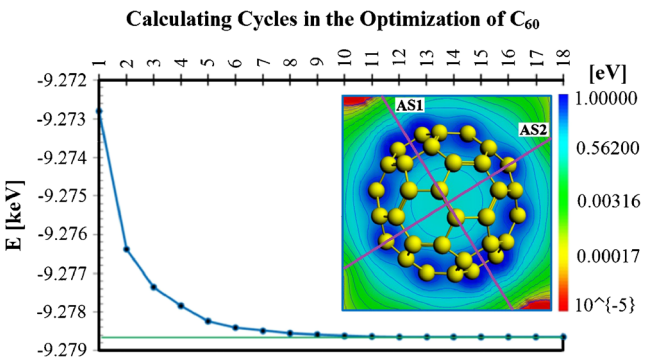


**Fig. 1** The graph shows the energy's convergence to the ground state during the geometrical optimization process for the fullerene $C_{60}$, inserted inside, the final configuration with the electric equipotential curves of the molecule and their intensity in a color scale

With this geometric optimization, we found for the configuration at ground state the correct distribution and length of single and double bonds. The average length of single bonds obtained was 1.45 Å and that of double bonds was 1.40 Å, which corresponds to the reported values [46] with a difference of less than ± 0.01 Å. The average carbon bond length (simple and double) is 1.44 Å.

Additionally, we performed the fullerene's molecular dynamics at 310 K (approximately human body temperature) and one atmosphere of pressure. The system presented a small oscillation of about ± 0.001 keV around the value of the total energy – 9275.9710 eV. The variation in the total energy with respect to the ground state corresponds to natural behavior in a system that thermally vibrates. The energy for molecular formation obtained was – 424.91 eV, where the average cohesive energy per atom is – 7.08 eV. It decreased with respect to the one found for the ground state by – 0.05 eV. This variation is extremely small (about 0.6 %) and is consistent with the fact that the fullerene does not experience significant changes from the ground state at 310 K, according to our calculations, the fullerene molecule is very stable in the temperature range of 0 K to 310 K. (In order to destroy the fullerene, temperatures greater than 1000 °C are necessary [47]).

### Optimization of $C_{60}$ containing $Na^{131}I$

With geometric optimization, we obtained 2.79 Å for the $Na^{131}I$ molecule ionic bond distance, which differs with respect to the reported value of [48] in ± 0.08 Å. This result allowed us to effectively use this method of calculation and the corresponding potential.

Using the $C_{60}$ fullerene's configuration previously obtained, $C_{60}$'s optimization was performed with one to three molecules of $Na^{131}I$ contained. The results found in the optimizations are presented in Table 1, which shows the system's formation energy, encapsulation energy per molecule of $Na^{131}I$ and carbon (single and double) bond length average.

As the sodium radio-iodide content increases, the fullerene expands and the geometric structure of $C_{60}$ is weakened. This increases the bond length between carbons and decreases the binding energy per atom. The average bond length became longer than the graphite bond type (≅ 1.42 Å), so that the stress

**Table 1** $C_{60}$ fullerene containing sodium radio-iodide geometrical optimization's results

| Optimization | $E_{nf}$ [eV] | $\Delta E_n$ [eV] | <d(C−C)> |
|---|---|---|---|
| $Na^{131}I@C_{60}$ | −423.03 | −13.64 | 1.45 Å |
| $2Na^{131}I@C_{60}$ | −407.20 | −12.72 | 1.48 Å |
| $3Na^{131}I@C_{60}$ | −380.60 | −11.53 | 1.51 Å |

in the structure increases as the structure weakens. The next set of graphs, of convergence to the lowest energy state, Fig. 2, shows the initial and final configuration states in the optimizations.

It can be inferred with the difference between initial and final state, during the geometrical optimization process, that $Na^{131}I$ molecules inside the fullerene change their initial positions that were determined with simple symmetry criteria. During the geometrical optimization process, as a function of calculation cycles, there is a plateau type behavior between calculating cycles 12–22 with $2Na^{131}I$ molecules contained in the fullerene, whereas a well behaved continuously progressive stabilization is observed for 1 and 3 $Na^{131}I$ molecules (see Fig. 2b). However, this apparent plateau actually is a continuous change of slope; this occurs because during the geometric optimization the fullerene contained molecules are in continuous rearrangement and although, in that interval, the two molecules of $Na^{131}I$ move perceptively because there is an interaction with the inner surface of fullerene, however, there still exists an instability, so that the convergence process continues until 64 step. The next graph, Fig. 3, shows energy changes in the range 12–22 of calculation cycles of $2Na^{131}I@C_{60}$.

The case where the fullerene's content exceeded three sodium radio-iodide molecules, i.e., ($4Na^{131}I$), was shown to be unstable, the structure cannot resist the expansion and breaks the fullerene allowing the release of the initially contained molecules in the nanocapsule, as shown in Fig. 4.

Figure 4 shows an intermediate state of the dissociating process of the system which initially consisted of a fullerene with four molecules of sodium radio iodide inside. The system broke and released the molecules contained inside, this instability may continue to change their shape and structure. The same goes for fullerenes initially containing a greater amount of $Na^{131}I$ molecules (5, 6, or 7), they break and become unstable systems, they may eventually reach a minimum energy state but radically will change the structure and will lose the encapsulation property which is of interest for our study.

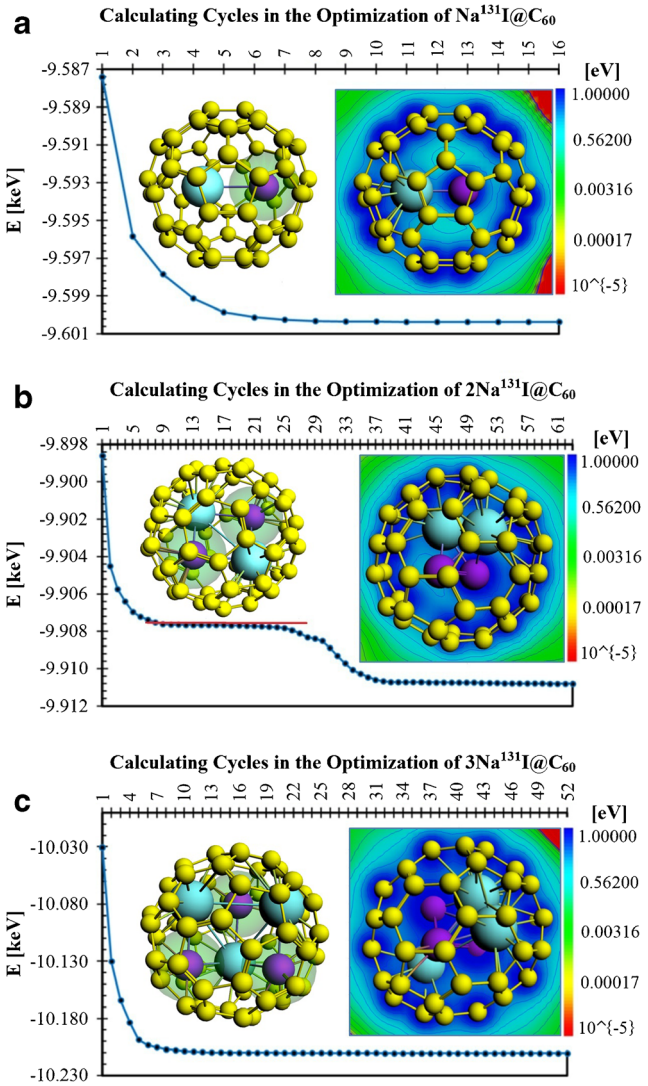


**Fig. 2** The graphs show the geometrical optimizations of the systems: a) $Na^{131}I@C_{60}$, b) $2Na^{131}I@C_{60}$, and c) $3Na^{131}I@C_{60}$, in each case the initial configuration (at left) and the final state (at right) are presented with the electric equipotential curves of the molecules showing their intensity in a color scale

## Charge distribution of $C_{60}$ containing $Na^{131}I$

Using the ADF code, based on the linear combination of atomic and molecular orbital method we have obtained the empty $C_{60}$ molecule's Mulliken electronegativity and, with 1 to 3 sodium radio-iodide molecules inside. Empty $C_{60}$ is practically neutral, as the sodium radio-iodide content rises, a "slight" shift of negative charges of the Mulliken population occurs from the iodine $^{131}I$ atoms toward the buckyball's carbon atoms, see Fig. 5. This produces some repulsion of the carbon atoms which explains why their binding energy diminishes, bonds become longer, and the structure is weakened.

The length of C−C bonds is larger when increasing the negative partial atomic charge on the carbons of the fullerene

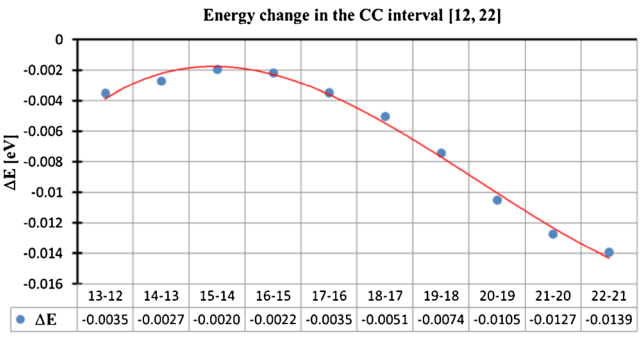


**Fig. 3** Energy change of the system $2Na^{131}I@C_{60}$ in the calculating cycles interval [12, 22]. The *red polygonal third grade trend curve* shows that the energy continuously changes in the interval

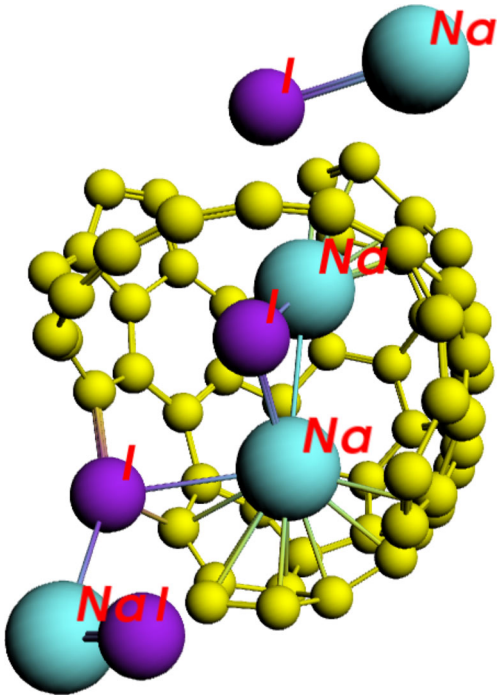


**Fig. 4** Instability of $4Na^{131}I@C_{60}$

and is shorter when the extra negative charge is lower. The same happens on average around the fullerene, as it increases its negative electric charge expands. These results are shown in Table 2.

While not always, usually the most charged atoms coupled have the longest bond and the tendency to lengthen the bond is clear as the electronegative charge increases. Similarly, the pairs of charged atoms with less charge present shorter bond lengths.

The case for which the fullerene molecules initially contains four $Na^{131}I$ shows a decrease of the average charge with respect to the case with three $Na^{131}I$ on the carbons of the fullerene, being −0.0808, however, this is at the expense of the structure of the fullerene.

## Molecular dynamics of $C_{60}$ containing $Na^{131}I$

Fullerene is a stable structure in temperature ranges lower than 900 K as has been proven in many works [49]: since the early observation of superconductivity by Hebard et al. [50] at $T_c$= 18 K of potassium-doped $C_{60}$ crystal until recent experimental and computational studies about the behavior of endohedral fullerene/noble gas systems, as well as the dynamics of fullerene systems and how they may encapsulate certain atoms and release them as function of high temperatures between 1000 and 4000 K [51].

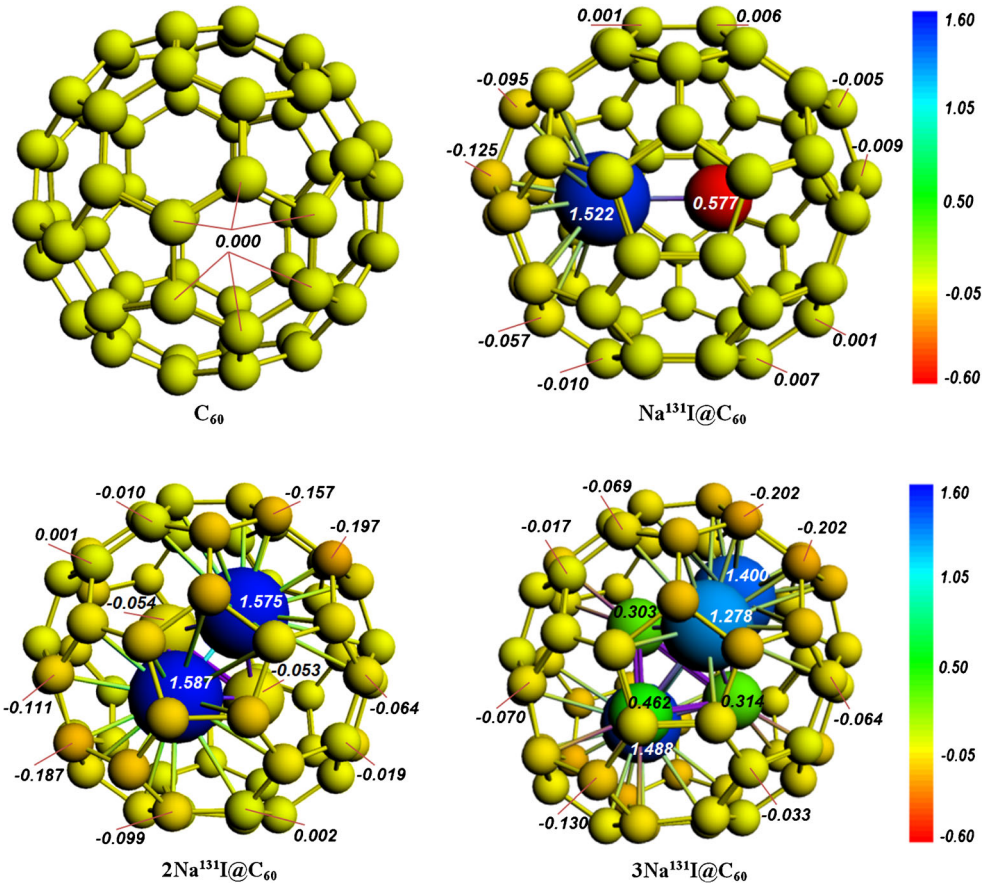


**Fig. 5** Electro negative charge distribution trend on the Mulliken scale of the empty $C_{60}$ and with one to three $Na^{131}I$ molecules inside

**Table 2** The average charge on carbons of fullerene, the average bond length, the maximum - $d_M$ - and minimum - $d_m$ - (C–C) bond length and their respective carbon charge averages for systems $nNa^{131}I@C_{60}$, $n$=1, 2, 3

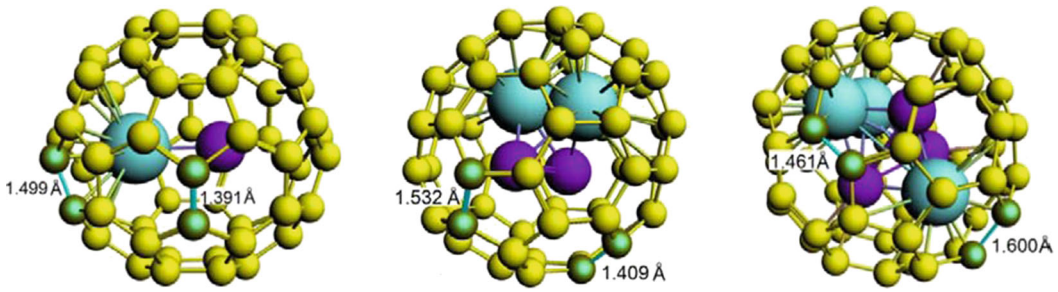


| System | $Na^{131}I@C_{60}$ | $2Na^{131}I@C_{60}$ | $3Na^{131}I@C_{60}$ |
|---|---|---|---|
| $<C_{Charge}>$ | − 0.0157 | − 0.0509 | − 0.0874 |
| $<d(C–C)>$ | 1.448 Å | 1.475 Å | 1.511 Å |
| $d_M(C–C)$ | 1.499 Å | 1.532 Å | 1.600 Å |
| $[d_M(C–C)]_{Charge}/2$ | − 0.1113 | − 0.0634 | − 0.1821 |
| $d_m(C–C)$ | 1.391 Å | 1.409 Å | 1.461 Å |
| $[d_m(C–C)]_{Charge}/2$ | 0.0033 | − 0.0042 | − 0.0371 |

For our purposes, which concern the uses of the nanocapsules with radioactive content inside the human body to employ like auxiliary in the cancer treatment, we are interested in the behavior of the nanocapsules at 310 K which is the approximate human body temperature. Molecular dynamics at 310 K and one atmosphere of pressure for $nNa^{131}I@C_{60}$, $n$=1, 2, 3 systems yield the results presented in Table 3.

The average binding energy per atom obtained in molecular dynamics at 310 K and one atmosphere of pressure for each system listed in the above table, differ by percentages of approximately 0.6 % of the average values obtained for ground state. Therefore, it is found that these systems have not changed significantly with the variation of temperature in the range 0 K to 310 K, as would be expected.

The study performed at this temperature range validates that this kind of nanocapsule can be used within a human body without temperature being a factor that can affect its stability. This result is consistent with those reported recently by Ghorbanzadeh Ahangari et al. [52].

**Table 3** Molecular formation energy and encapsulation energy per molecule of $Na^{131}I$

| Molecular dynamic | $E_f$ [eV] | $\Delta E_n$ [eV] |
|---|---|---|
| $Na^{131}I@C_{60}$ | −418.66 | −13.57 |
| $2Na^{131}I@C_{60}$ | −404.72 | −12.66 |
| $3Na^{131}I@C_{60}$ | −378.16 | −11.47 |

## Conclusions

The DFT geometrical optimizations and molecular dynamics performed with Quantum Espresso v.4.3 code presented in this paper make it possible to establish the feasibility of fullerene $C_{60}$ to store within itself, up to three $Na^{131}I$ molecules in an energetically stable form. The analysis of the Mulliken's electronegativity of the systems we have studied proves that a small fraction of the electrical charge of the iodine atoms is transferred to the carbon atoms of the fullerene. This causes the fullerene's expansion when its content of sodium radio-iodide molecules increases from one to three. We can conclude that these nanocapsules can be used as functional transporters for the treatment of tumors; but further testing is needed about surface adsorption properties of fullerenes containing radioactive sodium radio-iodide to anchor different atoms or compounds that will serve as molecular identifiers and allow guidance of nanocapsules to different malignant neoplasm tissue.

An interseting aspect to note is that the radioactive contents could be placed inside multilayer systems as the $C_{60}@C_{180}$

studied by Ghorbanzadeh Ahangari et al. [52]. For the latter it is possible that the nanocapsules will be more robust and will have more interaction properties with specific compounds to create radioactive doses.

**Acknowledgments** Special thanks to Consejo Nacional de Ciencia y Tecnología for the financial support given to this work and to NES Supercomputer Center of the Dirección General de Cómputo y de Tecnologías de Información y Comunicación, Universidad Nacional Autónoma de México, for their technical support on many of the computations performed.

## References

1. Ferlay J, Shin HR, Bray F, Forman D, Mathers C, Parkin DM (2010) Incidence/mortality data. GLOBOCAN 2008 v2.0. Cancer Incidence and Mortality Worldwide: IARC CancerBase No. 10 [Internet]. Lyon, France: International Agency for Research on Cancer. Available from: http://globocan.iarc.fr
2. Vicent S, Luis-Ravelo D, Antón I, Hernández I, Martínez S, de las Rivas J, Gúrpide A, Lecanda F (2006) Las metástasis óseas del cáncer. Anales del Sistema Sanitario de Navarra. Vol 29, No 2. http://lapica.cesca.es/index.php/ASSN/article/view/2566
3. Cleeland CS, Allen JD, Roberts SA et al (2012) Reducing the toxicity of cancer therapy: recognizing needs, taking action. Nat Rev Clin Oncol 9:471–478. doi:10.1038/nrclinonc.2012.99, http://www.nature.com/nrclinonc/journal/v9/n8/full/nrclinonc.2012.99.html
4. Bohunicky B, Mousa SA (2011) Biosensors: the new wave in cancer diagnosis. Nanotechnol Sci Appl 4:1–10. doi:10.2147/NSA.S13465
5. Bernholc J (1999) Computational materials science. The era of applied quantum mechanics. Phys Today 52(9):30–35. doi:10.1063/1.882840, http://scitation.aip.org/content/aip/magazine/physicstoday/article/52/9/10.1063/1.882840
6. ICMAB-CSIC. Methodologies for materials science and nanotechnology. http://icmab.es/research/research-lines#methodologies-for-materials-science-and-nanotechnology
7. Montellano A, Da Ros T, Bianco A, Prato M (2011) Fullerene $C_{60}$ as a multifunctional system for drug and gene delivery. Nanoscale 3(10):4035–4041. doi:10.1039/c1nr10783f
8. Liu Z et al (2007) Imaging the dynamic behaviour of individual retinal chromophores confined inside carbon nanotubes. Nat Nanotechnol 2:422–425
9. Koshino M et al (2007) Imaging of single organic molecules in motion. Science 316:853
10. Meyer RR et al (2000) Discrete atom imaging of one-dimensional crystals formed within single-walled carbon nanotubes. Science 289:1324–1326
11. Hong SY, Tobias G (2010) Filled glycosylated carbon nanotubes for in vivo radioemitter localization and imaging. Nat Mater 9:485–490. doi:10.1038/nmat2766
12. Iezzi EB et al (2002) Lutetium-based trimetallic nitride endohedral metallofullerenes: new contrast agents. Nano Lett 2:1187–1190
13. Koltover VK (2007) Endohedral fullerenes: from chemical physics to nanotechnology and nanomedicine. In: Lang M (ed) Progress in fullerene research. Nova, New York, pp 199–233
14. Ohtsuki T et al (1998) Insertion of Xe and Kr atoms into $C_{60}$ and $C_{70}$ fullerenes and the formation of dimers. Phys Rev Lett 81:967–970
15. Ivanovskaya VV, Köhler C, Seifert G (2007) 3d metal nanowires and clusters inside carbon nanotubes: structural, electronic, and magnetic properties. Phys Rev B 75:075410
16. Weck PF, Kim E, Czerwinski KR, Tomanek D (2010) Structural and magnetic properties of $Tc_n@C_{60}$ endohedral metalofullerenes. Phys Rev B 81:125448
17. Javan MB, Tajabor N, Rezaee-Roknabadi M, Behdani M (2011) First principles study of small cobalt clusters encapsulated in $C_{60}$ and $C_{82}$ spherical nanocages. Appl Surf Sci 257:7586
18. Javan MB, Tajabor N (2012) Structural, electronic and magnetic properties of $Fe_n@C_{60}$ and $Fe_n@C_{80}$ (n=2–7) endohedral metallofullerene nano-cages: first principles study. J Magn Magn Mater 324(1):52–59. doi:10.1016/j.jmmm.2011.07.034
19. Parr RG, Yang W (1989) Density-functional theory of atoms and molecules. Oxford University Press, New York, pp 76–77
20. Tereshchuk P, Da Silva JLF (2012) Encapsulation of small magnetic clusters in fullerene cages: a density functional theory investigation within van der Waals corrections. Phys Rev B 85(19), Article ID: 195461. doi:10.1103/PhysRevB.85.1954
21. Garg I, Sharma H, Kapila N, Dharamvir K, Jindal VK (2011) Transition metal induced magnetism in smaller fullerenes ($C_n$ for n≤36). Nanoscale 3(1):217
22. RadiologyInfo.org Terapia de yodo radioactivo (I-131) para hipertiroidismo. http://www.radiologyinfo.org/sp/info.cfm?pg=radioiodine
23. Pauwels EK, Smit JW, Slats A, Bourguignon M, Overbeek F (2000) Health effects of therapeutic use of $^{131}I$ in hyperthyroidism. Q J Nucl Med 44(4):333–339
24. Health Physics Society North Carolina Chapter. PO Box 37638, Raleigh NC 27627. Contact: NCHPS President Wendy Woehr. Nuclide Information Library. 131I. http://www.hpschapters.org/northcarolina/nuclide_information_library.php3
25. Kuo J (2013) Radioactive iodine ablation therapy: what to expect. New York Thyroid Center. Thyroid Cancer Awareness Month — September. http://cpmcnet.columbia.edu/dept/cs/thyroid/rai_what_to_expect.html
26. Kostarelos K (2008) The long and short of carbon nanotube toxicity. Nat Biotechnol 26(7):774–776. doi:10.1038/nbt0708-774
27. Poland CA, Duffin R, Kinloch I et al (2008) Carbon nanotubes introduced into the abdominal cavity of mice show asbestos-like pathogenicity in a pilot study. Nat Nanotechnol 3:423–428. doi:10.1038/nnano.2008.111
28. Kroto HW, Heath JR, O'brien SC, Curl RF, Smalley RE (1985) C(60): Buckminsterfullerene. Nature 318:162–163. doi:10.1038/318162a0
29. Dresselhaus MS et al (1996) Science of fullerence and carbon nanotubes. Academic, San Diego
30. Hohenberg P, Kohn W (1964) Inhomogeneous electron gas. Phys Rev 136:B864–B871
31. Perdew JP, Burke K, Ernzerhof M (1996) Generalized gradient approximation made simple. Phys Rev Lett 77:3865–3868
32. Marx D, Hutte J (2000) Modern methods and algorithms of quantum chemistry. In: Grotendorst J (ed) NIC series, vol 1. John von Neumann Institute for Computing, Jülich, pp 301–449
33. Giannozzi P, Baroni S, Bonini N, Calandra M, Car R, Cavazzoni C et al (2009) Quantum ESPRESSO: a modular and open-source software project for quantum simulations of materials. J Phys Condens Matter 21:395502–395519
34. Perdew JP, Zunger A (1981) Self-interaction correction to density-functional approximations for many-electron systems. Phys Rev B 23:5048–5079
35. Giannozzi P (2007) Notes on pseudopotential generation. Scuola Normale Superiore di Pisa
36. Troullier N, Martíns JL (1991) Efficient pseudo potentials for plane-wave calculations. Phys Rev B 43:1993–2006
37. Gonze X, Kackell P, Scheffler M (1990) Ghost states for separable, norm conserving, ab initio pseudo potentials. Phys Rev B 41:12264–12267
38. Monkhorst HJ, Pack JD (1976) Special points for Brillouin-zone integrations. Phys Rev B 13:5188–5192
39. Fernández-Torre D, Kupiainen O, Pyykkö P, Halonen L (2009) Long-range interactions between polar molecules and metallic

surfaces: a comparison of classical and density functional theory based models. Chem Phys Lett 471:239–243
40. Rangel E, Vázquez G, Magaña F, Sansores E (2012) Interaction between an icosahedron Li(13) cluster and a graphene layer doped with a hydrogen atom. J Mol Model 18(12):5029–5033. doi:10.1007/s00894-012-1504-2
41. Parrinello M, Rahman A (1981) J Appl Phys 52:7182
42. Bethune DS, Johnson RD (1993) Atoms in carbon cages: the structure and properties of endohedral fullerenes. Nature 366(6451):123–128. doi:10.1038/366123a0
43. Tomanek D, Wang Y, Ruoff RS (1993) Stability of fullerene-based systems. J Phys Chem Solids 54(12):1679–1684
44. Cioslowski J, Nanayakkara A (1992) Phys Rev Lett 69:2871
45. Hua X, Cagin T, Che J, Goddard WA III (2000) QM(DFT) and MD studies on formation mechanisms of $C_{60}$ fullerenes. Nanotechnology 11:85–88
46. Hare J et al Some properties of carbon and $C_{60}$. Brighton, East Sussex BN1 9QJ. http://www.creative-science.org.uk/propc60.html. Accessed January 2013
47. Becker L, Poreda RJ, Bunch TE (2000) Fullerenes: an extraterrestrial carbon carrier phase for noble gases. Proc Natl Acad Sci U S A 97(7):2979–2983
48. Nave CR Properties of ionic diatomic molecules. HyperPhysics http://hyperphysics.phy-astr.gsu.edu/hbase/tables/diatomic.html#c1. Accessed June 2013
49. Yamaguchi Y, Maruyama S (1998) A molecular dynamics simulation of the fullerene formation process. Chem Phys Lett 286:336–342
50. Hebard F, Rosseinsky MJ, Haddon RC, Murphy DW, Glarum SH, Palstra TTM, Ramírez AP, Kortan AR (1991) Superconductivity at 18 K in potassium-doped $C_{60}$. Nature 350:600
51. Tilton P, Suchy B, Balasubramanya MK, Roth MW. Simulated dynamics and endohedral relesase of Ne from Ne@$C_{60}$ clusters. Under review. http://www.researchgate.net/publication/1883212_Simulated_Dynamics_and_Endohedral_Relesase_of_Ne_from_NeC60_Clusters
52. Ghorbanzadeh Ahangari M, Fereidoon A, Darvish Ganji M, Sharifi N (2013) Density functional theory based molecular dynamics simulation study on the bulk modulus of multi-shell fullerenes. Phys B Condens Matter 423:1–5